

# Tactile After-Images at Low Temporal Frequency \*

U. Singh, R.S. Fearing  
 Department of EE&CS  
 University of California  
 Berkeley, CA 94720-1770

## Abstract

A stimulator display for the human tactile system needs to make use of both the spatial and temporal characteristics of the sense of touch. The temporal response of the human tactile system includes viscoelastic memory. We ran psychophysical experiments on human subjects to determine whether the finger exhibits a significant amount of viscoelastic memory and how this affects the overall tactile system. Since most tactile stimulators include an elastic layer as an anti-aliasing filter, our tests were carried out with a layer of elastic material on the finger. There was a significant amount of memory in the finger which affected the perception of the inputs presented to the subjects. We offer a possible explanation for the results based on the mechanics of the skin.

## 1 Introduction

In the visual world, terms such as refresh rates and frames/sec define the bandwidth of a visual display system. TVs and monitors are built to use the well known limitations of our visual system (*e.g.* interlaced scanning, minimum refresh rate of  $70\text{Hz}$  for flicker free displays). This same principal can be applied to tactile display. If we had more information about the human tactile system, we could use it to build better displays (*e.g.* use interlaced scanning of the pins across the finger by using the memory in the finger). This paper tries to determine the limitations in dynamic human tactile perception that could be used to improve tactile display resolution.

Neurophysiological studies by LaMotte and Srinivasan (1987) suggest that SAI mechanoreceptors are most important in small-scale shape perception. The SAIs have a field diameter of  $3-4\text{mm}$ , a frequency range of  $DC-30\text{Hz}$  and sense local skin curvature [10]. This suggests that a relatively low bandwidth display might work for most applications. The SMA actuated display designed by Kontarinis has a bandwidth with a  $-3\text{dB}$  point between  $6-7\text{Hz}$  [10]. Cohn et al. get a  $7\text{Hz}$  frequency response out of their pneumatically actuated display. Both of these displays are well below the  $30\text{Hz}$  bandwidth of the SAI mechanoreceptor. Since there are some physical limitations (such as hysteresis in SMA), display bandwidths might not increase in the near future (recently  $50\text{Hz}$  bandwidth was achieved using SMA with ice water cooling [7]). But performance improvements can still be made by exploiting the perceptual properties of the human finger.

This project attempts to determine if the viscoelasticity of the finger creates a tactile after-image in human tactile

perception. We use a similar setup as Tan [19] and conduct psychophysical experiments to determine if the viscoelastic memory can be quantitatively observed in human subjects. We also present a model to explain how this memory affects overall tactile perception.

### 1.1 Previous work

Many researchers have examined the mechanical properties of skin. Pawluk and Howe have used Fung's quasi-linear viscoelastic model of tissue to propose a viscoelastic model which describes the response of the human finger pad to mechanical deformation [14], [13]. They also showed that the finger pad can be described by a non-linear relationship between force and stiffness. Much of this work has also been done by Fung for soft tissues [6]. Serina, Mote and Rempel have done studies on finger pad displacement for ergonomic purposes. They have shown that the bone, nail interface can be considered incompressible compared to the finger pad [13].

There has been very little work done with temporal response of the human tactile perception. We could not find any work that dealt with *viscoelastic memory* in the human finger and how this affects the tactile perception. There has been some work done by VanDoren with spatio-temporal sensitivity [2]. This model treats the finger pad as a linear Voigt body. The model he presents is valid for very low forces ( $0.1\text{N}$ ). Verrillo and Chamberlain, as discussed by VanDoren, have done some temporal studies with the tactile system. But their work focuses on inputs with frequencies of  $250\text{Hz}$  and higher [3]. Tan's research to determine spatial sensitivity of the human finger was affected by temporal properties of the finger. In his experiments, subjects reported that, after wearing the rubber gloves (anti-aliasing elastic layer) for some time, patterns became harder to discern. Some subjects claimed that they perceived grating patterns on two comparison surfaces, when in fact one was known to be smooth. Although he did not draw any quantitative conclusions, he hypothesized that the viscoelastic memory of the finger might be confusing the SAI mechanoreceptors. He states that the amplitude resolution capabilities of the human finger might be decreased by the viscoelastic memory causing errors in perception [19].

## 2 Experimental Methods

### 2.1 Apparatus

We developed a system where patterns could be presented to test subjects in a controlled manner using the robot modules of the Robotworld system. We used a Lord

\*This work was funded in part by: NSF grant IRI-9531837.

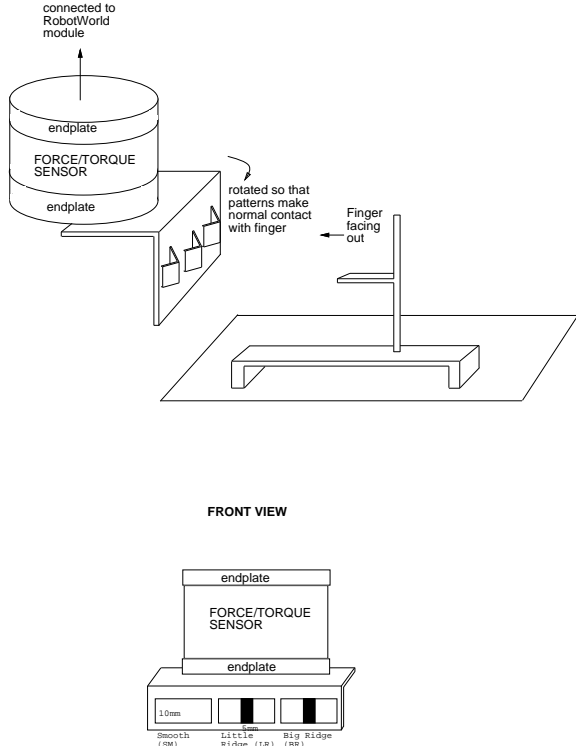


Figure 1: Testing apparatus

15/50 Force/Torque sensor directly attached to the robot module. There were also two momentary switches (as well as accompanying real-time device drivers) placed within easy reach of the apparatus to record the responses of the subjects. The entire apparatus was hidden from the view of the test subject. For each of the procedures outlined in section 2.2, the subject had his or her right index finger on a ledge with the palm of the hand facing towards the module. The module moved a plate containing wax blocks towards the finger. The robot module moved the plate until a block came in contact with a subject’s finger pulp. The plate, blocks, and the rubber fingertip are described in the sections below. Figure 2.1 shows the complete apparatus used during the experiment.

### 2.1.1 Patterns

The patterns presented to the subject consisted of machinable wax blocks with a ridge milled onto its surface. The heights of the ridge varied from  $0.1mm$  to  $1.5mm$ . Each ridge on the different blocks had a width of  $5mm$  (figure 2.1) and the blocks came in contact with the finger in such a way that the length of the contact along the ridge was approximately  $10mm$  (figure 10). There were also blocks that had no ridges (again the contact length on the finger was  $10mm$ ). Note, we used a stair-step configuration on the plate to ensure that the blocks had normal contact with a subject’s finger and at the same time only the block being presented came in contact with the finger pulp. During a test, the index finger of the subject was placed on a ledge with the pulp facing out (so that the nail rested against the back of the ledge).

### 2.1.2 Rubber glove

A  $2.0mm$  thick rubber glove was fitted on the index finger of each subject. The gloves were manufactured with silicone rubber using the process described in [19].

The wax blocks that were presented as inputs to a subject’s finger had varying textures and different thermal signatures. Without a rubber glove, one could obtain additional information from these surface texture and temperature cues.

In one set of experiments, one of the inputs was a wax block with ridge heights of  $0.1mm$  or  $0.15mm$  (called little ridge input). We wanted the little ridge input to be ambiguous (i.e. at a 50% threshold level) to perceive for our experiments. Without the rubber glove, the ridge heights would have to be much lower than  $0.1mm$  (making them very difficult to manufacture) for the little ridge inputs to be perceived as ambiguous.

## 2.2 Procedure

We measured the finger’s dynamic response. We applied a position step to the finger and measured the finger’s force response (this is defined to be the relaxation function). The robot module was commanded to a position that corresponded to a force of  $2.5N$  (measured by the force/torque sensor) exerted on the finger by the block containing the biggest ridge (this corresponded to blocks with ridge heights of  $0.7mm$  or  $1.0mm$ ). After fifteen seconds, during which the force response of the finger was recorded by the sensor, a position step of  $0.05cm$  towards the finger was applied by the robot. The force/torque sensor recorded the force for thirty seconds. Finally, the module was commanded to move back to its original position (i.e. a negative step of  $0.05cm$ ) and the sensor recorded the force for another fifteen seconds. Due to the limited velocity of the robot module, the position step was not instantaneous. It took on the order of  $0.6 - 0.7seconds$  to move the  $0.05cm$ . The above procedure gave us a relaxation curve for each subject. The results and analysis are discussed in section 3.

### 2.2.1 Effect on Tactile Perception

In the second part of the experiment, we determined if the viscoelasticity of the finger pulp had a statistically significant effect on the perception of ridges on the wax blocks. The plate was set up with three blocks. The leftmost block (in figure 2.1) was smooth (SM) block (had no ridge). The middle groove contained a block with a little ridge (LR) whose height was either  $0.1mm$  or  $0.15mm$ . The height of the LR for each subject was determined before the experiment started. It corresponded to the ridge height that was just at threshold through the  $2.0mm$  glove. The threshold point was defined to be the ridge height at which the subjects were guessing whether they had felt a ridged pattern (i.e. there was equal chance of a subject guessing that he/she had felt a smooth pattern). The third groove on the plate in figure 2.1 had the block containing a big ridge (BR). The BR block was the same as the block used in the viscoelastic test (2.2) to measure the relaxation function of a subject. The robot module was commanded to move the plate to the finger until the block being presented as stimulus applied a force of  $5.5N$  on the finger (as measured by the force/torque sensor). The ordering and the timing

Type	First Stimulus	Second Stimulus
1	SM	BR
2	SM	SM
3	BR	SM
4	LR	BR
5	BR	LR

Table 1: Trial types and corresponding patterns presented (SM=Smooth, LR=Little Ridge, BR=Big Ridge).

Choice/Button	Condition(s)
1	Neither input had ridges,
	Only one input had ridge,
	Input(s) had negative ridges (grooves)
2	Both inputs in the trial had positive ridges

Table 2: Choices and condition(s) for each choice

of stimulus was controlled very carefully and is described below.

The experiment consisted of 150 trials broken up into five sessions (thirty trials per session). Each trial consisted of two blocks being presented to the subject. Each trial was one of five types outlined in the table 1. Note, with three different blocks, each trial could have been one of nine ( $3^2$ ) different types (since two blocks were being presented in each trial). But we only used the combination of blocks that were important (to cut down on the number of trials) in showing whether or not the viscoelasticity of the finger had an effect on touch. The set of 150 trials was generated randomly prior to the experiment. They were generated in such a way that there was a set of thirty trials of each type in the experiment. Thirty trials were picked because the normal approximation (using the central limit theorem) is a good approximation regardless of the shape of the population if the sample size is greater than or equal to thirty [20]. Furthermore, since the experiment was carried out over five sessions (a session consisted of thirty trials), each session had six trials of each type.

In each trial, the robot module presented the first stimulus with a force of  $5.5N$  for exactly 3 seconds at which point the module moved away from the finger and waited for exactly 1.8 seconds (1.8 was picked because it was determined from the first experiment that the average relaxation time constant for the subjects was approximately 2 seconds). Following the wait, the second stimulus was presented (also at  $5.5N$ ) for exactly 2 seconds. The subjects were asked to push the appropriate button (momentary switch) based on whether or not they felt two ridges in the trial (i.e., felt ridges on both the stimuli). The conditions for when the subjects were supposed to push each button is outlined in table 2. The subjects had 10 seconds within which to make a choice. In other words, the time between each trial was held constant at 10 seconds. The results were compiled and are analyzed in section 3.

### 3 Results

The experiments were run on six test subjects, 3 male and 3 female. All subjects were volunteers and no spe-

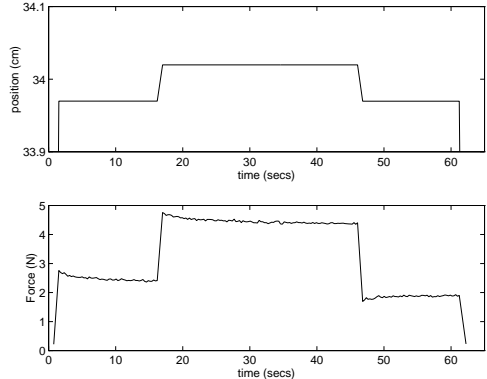


Figure 2: Relaxation function for a rubber layer.

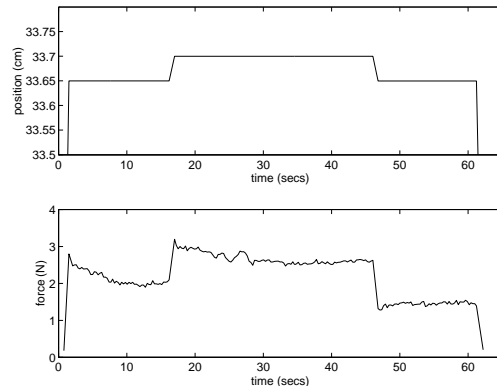


Figure 3: Relaxation function for one of the subjects (subject 2).

cial criteria were used to select them. Two subjects were familiar with the experimental apparatus and procedure, while the other four subjects had no prior knowledge. The ages of the subjects varied from 21 to 35 years of age. The following is the performance and analysis of each of the six subjects.

#### 3.1 Viscoelasticity

We showed in section 4.1 the finger mechanical model consisting of springs and dashpots. After running the first experiment, a relaxation function was obtained for each of the six subjects. Figure 2 shows a relaxation function (to a position step) for a rubber layer. Note, one can see a very small viscoelastic effect here. Figure 3 shows a relaxation function for one of the subjects (subject 2). The viscoelastic effect is very apparent up to approximately 15 seconds (just before the  $0.05cm$  position step). The other subjects exhibited similar relaxation functions. The relaxation function for the Kelvin, equation 6, can be rewritten more generally as

$$k(t) = A + Be^{-tc} \quad (1)$$

where  $A = E_R$ ,  $B = \frac{-E_R(\tau_\epsilon - \tau_\sigma)}{\tau_\epsilon}$ , and  $c = \frac{1}{\tau_\epsilon}$ . We used MATLAB (using a nonlinear curve fitting algorithm based on the simplex algorithm) to fit an exponential function of the form given in equation 1 to the force response taken in the first 15 seconds for each subject. Figure 4 shows an

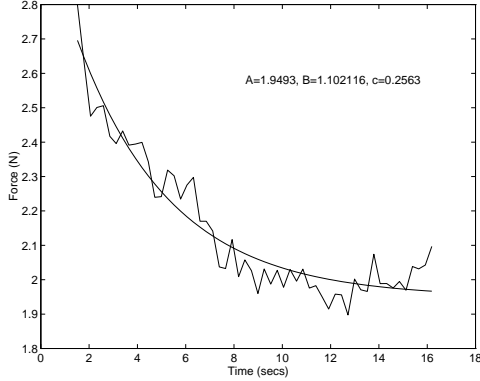


Figure 4: Exponential fit for relaxation function.

Subject	A	B	c	$\tau_\epsilon$	$\tau_\sigma$
1	2.29	1.15	0.70	1.42	2.14
2	1.95	1.10	0.26	3.90	6.11
3	2.20	0.89	0.58	2.71	3.82
4	2.24	0.67	0.35	2.81	3.65
5	2.04	0.85	0.30	3.38	4.78
6	2.59	0.34	0.26	3.88	4.39

Table 3: Parameter values of the viscoelastic model of the finger

example of the curve fitting for the relaxation curve of the subject shown in figure 3 which corresponds to subject 2. The data for the other subjects is shown in table 3. Note, the value  $\tau_\sigma$  can be found by substituting the known values into the equation for B in equation 1.

According to equation 7, and figure 8, after the constant force input is removed, the finger pulp (because of the viscoelastic creep) exponentially deforms back to its original location, with time-constant equal to  $\tau_\sigma$  (we will ignore all other constants for this analysis). When a BR pattern is pressed against the finger with a force of 5.5N for 3 seconds, then the deformation is equal to one (arbitrarily normalized units-zero corresponds to the finger pulp in its original location). 1.8 seconds after the pattern is removed, the finger will be at some position depending on the value of  $\tau_\sigma$  for each subject. Table 4 shows the deformation (in the above normalized units where zero corresponds to the finger in its original location, and one corresponds to the location of the finger after a BR pattern has been pressed on it for 3 seconds) for each subject 1.8 seconds after the BR pattern is removed. A smaller number means that the finger is closer to its original location. In other words, subject 1’s finger pulp is only 43% away from its starting location, whereas subject 2’s finger pulp is 74% from its original location. Equivalently, we can think of this as the finger pulp retaining some memory of the input even after 1.8 seconds. The first subject’s finger remembers 43% of the input while the finger on the second subject remembers 74% of the input.

### 3.2 Effect on perception

The second experiment was run on all six subjects. As mentioned earlier, the responses of the second experiment

Subject	Position of finger
1	0.43
2	0.74
3	0.62
4	0.61
5	0.69
6	0.66

Table 4: Position of finger 1.8 seconds after a BR pattern is applied (in normalized units where zero corresponds to finger in starting location, and one corresponds to location of finger after a BR pattern has been pressed on it for 3 seconds)

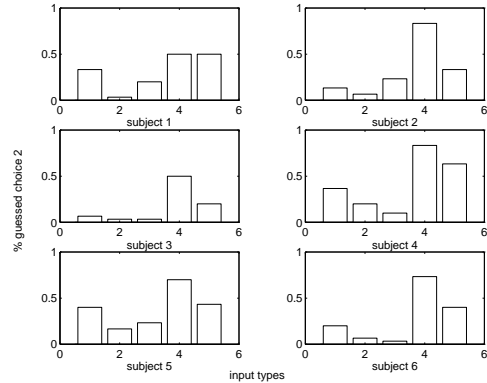


Figure 5: Fraction of trials of all types (1=(SM,BR), 2=(SM,SM), 3=(BR,SM), 4=(LR,BR), 5=(BR,LR)) for which ‘felt two ridges’ (choice 2) was picked as a response.

were either *choice1* (if a subject did not feel a ridge on each of the two inputs of the trial) or *choice2* which corresponded to a subject feeling two ridges in the trial (see table 2). The performance, as indicated by fraction of trials that a subject picked *choice2* for each type of trial, is shown in figure 5. Refer to table 1 to see what input patterns were presented for each type.

Looking at figure 6, we see that for trials of types 4 and 5, the fraction of trials for which subjects picked *choice2*, seems to be different. What we needed to determine is whether or not the difference in the the two fractions was statistically significant. In other words, what was the confidence level with which we could say that the means (fractions) of the response of *choice2* were different for each of the trial types. To accomplish this, we used a modified pooled *t*-test (sometimes called the two sample *t*-test). The pooled *t*-test is often used when comparing two means whose variances are unknown but equal. In our case, we wanted to compare the mean response of *choice2* for trials of type 4 ( $p_1$ ) and type 5 ( $p_2$ ) for each subject. The variance of *choice2* responses for type 4 was not equal to the variance of the responses for type 5. Thus, we had to use a modified pooled *t*-test which is described in section 3.2.1.

#### 3.2.1 Statistical Comparison of Means

We want to show that  $p_1$ , which is equal to the mean for type 4 inputs (in other words, it is the fraction of trials of

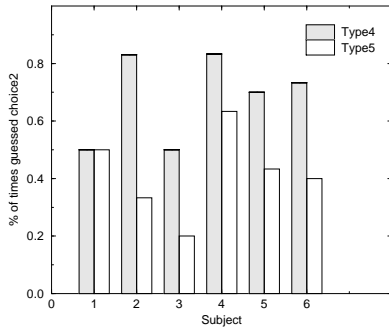


Figure 6: Fraction of trials of types 4 (LR,BR) and 5 (BR,LR) for which ‘felt two ridges’ (choice 2) was picked as a response

type 4 for which the response was *choice2*), is not equal to mean for type 5 inputs ( $p_2$ ). We also wanted to see if we could state this with 95% confidence interval for each of the subjects.

We begin by formulating the null hypothesis ( $H_0$ ) and the alternative hypothesis ( $H_1$ ). We know that a firm conclusion can only be made if a hypothesis is rejected. We would like to say that  $p_1 \neq p_2$ , or in other words, we would like to reject the hypothesis that  $p_1 = p_2$ . Therefore, in our case we form the null hypothesis and alternative hypothesis as outlined in equation 2.

$$\begin{aligned} H_0 : p_1 - p_2 &= 0 \\ H_1 : p_1 - p_2 &\neq 0 \end{aligned} \quad (2)$$

The two-sample  $t$ -test may be used when we can assume that both distributions are normal (which is a valid assumption in this case because the number of samples equals thirty which implies we can use the central limit theorem). In our case, we have two means, but we do not have the variances. Furthermore, we can safely assume that the variances of each of the distributions are not equal. Therefore, we use the modified two-sample  $t$ -test which uses sample variances. The sample variance can be calculated for the distribution of responses for type 4 and type 5 trials as outlined in equation (3).

$$\sigma^2 = \frac{\sum_{i=1}^n (x_i - \bar{x})^2}{n - 1} \quad (3)$$

The value of the test statistic is given by equation 4

$$t' = \frac{\bar{x}_1 - \bar{x}_2}{\sqrt{\frac{\sigma_1^2}{n_1} + \frac{\sigma_2^2}{n_2}}} \text{ and } \nu = \frac{(\frac{\sigma_1^2}{n_1} + \frac{\sigma_2^2}{n_2})^2}{\frac{(\sigma_1/n_1)^2}{n_1-1} + \frac{(\sigma_2/n_2)^2}{n_2-1}} \quad (4)$$

The means, sample-variances, and  $t$ -values for each subject are shown in table 5.

The critical region for the test is defined by equation (5) where  $\alpha$  is the probability of a type I error (i.e. rejection of the null hypothesis when it is true). It is also referred to as the level of significance.

$$\begin{aligned} t' &< -t_{\alpha/2} \\ t' &> t_{\alpha/2} \end{aligned} \quad (5)$$

Sub	Type	% Two ridges felt	$\sigma^2$	t-val	$\nu$
1	4 (LR-BR)	0.50	0.26		
	5 (BR-LR)	0.50	0.26	0	58
2	4 (LR-BR)	0.83	0.14		
	5 (BR-LR)	0.33	0.23	4.48	55.1
3	4 (LR-BR)	0.50	0.26		
	5 (BR-LR)	0.20	0.17	2.52	55.3
4	4 (LR-BR)	0.83	0.14		
	5 (BR-LR)	0.63	0.24	1.77	54.5
5	4 (LR-BR)	0.70	0.22		
	5 (BR-LR)	0.43	0.25	2.13	57.6
6	4 (LR-BR)	0.73	0.20		
	5 (BR-LR)	0.40	0.25	2.72	57.4

Table 5: Raw data and  $t$ -values for each subject

At a level of significance of 0.05 (i.e. 95% confidence level), we can determine the critical values of the  $t$ -distribution. For our values of  $\nu$  and  $\alpha$  equal to 0.05, it was determined that the critical value  $t_{\alpha/2}$  was equal to approximately 2.000. At a significance level of 0.10, the critical value was equal to 1.671. From this we can safely conclude that the means for trials of types 4 and 5 were not equal for subjects 2, 3, 5, and 6. Subject 4 fell within the 0.10 level of significance. Subject 1’s means were equal. This data is explained in section 5.

## 4 Models

### 4.1 Viscoelastic model of skin tissue

Fung concludes [6] that biological tissues are not elastic. The history of strain affects the stress (*viscoelastic memory*). There is a considerable difference in stress response to loading and unloading. This has led to work in characterizing soft tissues using linear viscoelastic models. Most of the research has concentrated on relating stress and strain in the soft tissue using Voigt, Maxwell, and Kelvin models [6].

The Kelvin model (also known as the standard linear model) is the most general relationship that includes the load, the deflection, and their first derivatives. We decided to use the Kelvin model to explain the viscoelastic behavior of the human finger pulp. The Kelvin model is shown in the figure 7. It consists of a series connection of a dashpot (with viscosity  $R$ ) and a spring (with spring constant  $k_1$ ) in parallel with another spring (with spring constant  $k_0$ ). Using the analysis in [6], we obtain the relaxation function (force response  $k(t)$  for a unit-step deformation)

$$k(t) = [E_R - \frac{E_R(\tau_\epsilon - \tau_\sigma)}{\tau_\epsilon} e^{-\frac{t}{\tau_\epsilon}}]1(t) \quad (6)$$

where  $\tau_\epsilon$  (called the *relaxation time for constant strain*),  $\tau_\sigma$  (*relaxation time for constant stress*), and  $E_R$  (*relaxed elastic modulus*) are all functions of  $R$ ,  $k_0$ ,  $k_1$ .

The form of the relaxation function is shown on the left in figure 8. The creep function (elongation produced by a application of a unit-step force  $F(t) = 1(t)$  for the Kelvin model is shown on the right in figure 8 and is represented

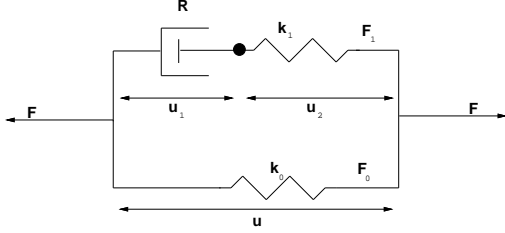


Figure 7: A Kelvin body (a standard linear solid).

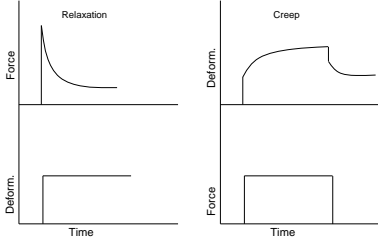


Figure 8: Relaxation and creep function for a Kelvin body.

by equation 7.

$$c(t) = \left[ \frac{1}{E_R} - \frac{(\tau_\sigma - \tau_\epsilon)}{E_R \tau_\sigma} e^{-\frac{t}{\tau_\sigma}} \right] 1(t) \quad (7)$$

## 5 Discussion

### 5.1 Skin Viscoelasticity and Perception

If there were no perceptual “after image”, there should be no effect of presentation order on detecting two ridges. However, all of our subjects but subject #1 showed a statistically significant difference in means between the (LR,BR) and (BR,LR) presentation order. Feeling the big ridge first reduced the probability of feeling the little ridge.

It is worthwhile to consider the relation between the measured viscoelastic properties and these perceptual results. Table 4 quantifies the non-elastic component of each subject’s finger response, i.e. the exponential term in eq. 7. The effect on perception is “measured” as the difference between the mean number of times two positive ridges were felt for type 4 trials (LR,BR) and type 5 trials (BR,LR). This can be thought of as a measure of memory in tactile perception. Figure 9 shows the strong correlation (correlation coefficient  $\rho = 0.92$ ) between slow skin relaxation and perceptual interference.

Subject 1 retains the least amount of finger deformation (only 43%) and also shows no problem with detecting both ridges with this experiment’s time scale. It is interesting to speculate that the relatively small amounts of viscoelasticity seen in subject 1 were compensated at the perceptual level.

### 5.2 Skin Mechanics and Tactile Memory

Although we do not have a very realistic model for the actual contact stresses and subsurface strains in the LR and BR cases, we can speculate as to why the LR is more difficult to feel after the BR contact. Our zeroth order model is that the tactile after-image is simply a scaled remanent of the previous contact, and finger strain is:

$$\epsilon(x) = \epsilon_{lr}(x) + \alpha(t)\epsilon_{br}(x), \quad (8)$$

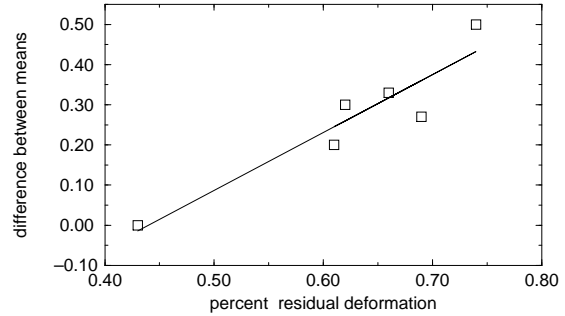


Figure 9: Difference in mean detection of 2 ridges in (LR,BR) and (BR,LR) versus percent residual deformation 1.8 seconds after BR input.

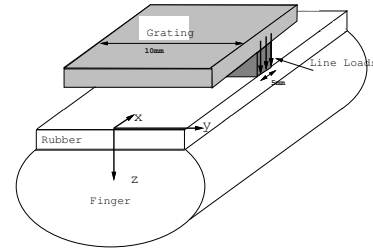


Figure 10: Finger and pattern geometry for plane stress assumption

where  $\epsilon_{lr}$  and  $\epsilon_{br}$  are subsurface strain for LR and BR contacts respectively, and  $\alpha(t)$  represents the amount of influence that the previous BR pattern has on the strain profile of the LR pattern. As an estimate for  $\alpha(1.8)$ , we chose to average the values of table 4.

As we have a large variation in subject finger size, shape and stiffness, as well as manufacturing variations in ridge edges, one needs to make some simplifying assumptions to provide rough comparisons of what strain the finger mechanoreceptors could be measuring for the smooth (SM), little ridge (LR) and big ridge (BR) contacts. We use the plane stress model for convenience (Figure 10) and reasonable fit to mechanoreceptor response [15]. The stresses due to contact with a raised ridge are modeled as normal line loads. They are constant in the y-axis (between 0 and 10mm in y-contact length). While this model is grossly simplified, it is qualitatively useful as a starting point for analysis. Better models of finger mechanics such as Srinivasan and Dandekar [18] are available, but the low-pass nature of the 2mm glove hides model details.

For a line load  $P$ , the normal component of strain is [9]:

$$\epsilon_z = \frac{-2Pz}{E\pi r^4} (z^2 - \nu x^2) \quad (9)$$

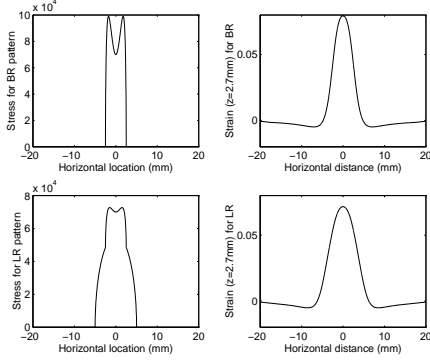


Figure 11: Approximate surface stress and sub-surface strain for big ridge (BR) and little ridge (LR).

where  $P$  is the force per unit length (N/m),  $r^2 = x^2 + z^2$ ,  $\nu$  is Poisson's ratio (0.5 for incompressible materials such as rubber), and  $E$  is  $4 \times 10^5 \text{ N/m}^2$  for our rubber layer. The pattern is pressed against the finger with a force of  $5.5 \text{ N}$  over a contact length of  $10 \text{ mm}$ , thus  $P = 550 \text{ N/m}$ .  $z$  is taken to be  $2.7 \text{ mm}$  (which corresponds to the  $2.0 \text{ mm}$  rubber layer thickness and an assumed  $0.7 \text{ mm}$  depth of the SAI mechanoreceptors in the skin). The actual depth of mechanoreceptors in humans is unknown and is probably quite variable.

For a smooth contact (SM), we assume [9]:

$$\sigma_z = \frac{2P}{\pi a^2} \sqrt{a^2 - x^2} \quad (10)$$

where  $a$  is the half width of the contact. A rectangular pattern has stress: [9]:

$$\sigma_z = \begin{cases} \frac{P}{\pi \sqrt{a^2 - x^2}} & \text{for } |x| < a, \\ 0 & \text{otherwise} \end{cases} \quad (11)$$

The BR pattern had its edges slightly smoothed, therefore we assumed a slight smoothing function applied to eq. 11. The LR pattern had a central region where contact is with the little ridge, and an outer region where contact was with the base of the wax block. As a crude approximation, we assumed superposition applied, and combined a rectangular response over the 5 mm ridge width with a smooth response over the 10 mm block. All contact stresses were scaled to ensure that the total load was 5.5 N. The assumed stress and strain profiles for the BR and LR patterns are shown in figure 11.

As shown in Figure 12, the smooth (SM) and little ridge (LR) contacts give quite similar strain profiles, while the big ridge (BR) contact is quite different from the SM contact. Thus subjects had no trouble perceiving the big ridge. As the LR contact is only perceived as a ridge 50% of the time, any remanent strain from a previous BR contact will have a significant effect on perception of the LR. Figure 13 shows the sub-surface strain for trials of type 5 (i.e. LR pattern applied 1.8 seconds after the BR pattern). In the figure,  $\alpha(1.8) = 0.6$ . The figure also shows the strain at  $z = 2.7 \text{ mm}$  for the LR pattern and a BR pattern. Looking at the strain profiles, it seems that the BR,LR profile would not feel like the LR or the BR profiles, which agrees with subjective impressions. Of course,

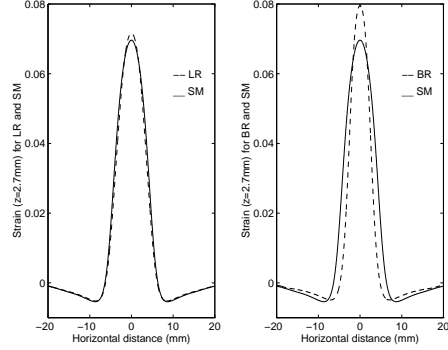


Figure 12: Sub-surface strain for ridged and smooth patterns

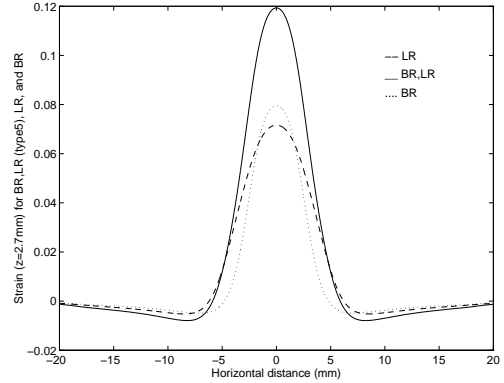


Figure 13: Sub-surface strain for LR, BR and after the second input for type5 (BR,LR) trial at  $t=1.8$  seconds

the residual strain from the BR contact will be decreasing, while the strain from the LR contact will be increasing during the contact interval.

### 5.3 Sources of Error

There were weaknesses in the experimental apparatus which lead to errors or inconsistencies in the data. The Lord Sensor, with no forces or load on it, had errors up to  $0.4N$  while measuring force. In fact, for one subject the standard deviation of the forces applied during the second experiment was  $1.5N$ . Inadvertent finger motion, giving high-frequency information from slip, was a potentially significant problem. In the interest of subject comfort, fingers were not completely immobilized. (If there is slipping during contact, then the FAI and FAII mechanoreceptors are stimulated.)

There were several limitations in the models we used. Fung [?], and Pawluk [?] have shown that the finger pulp behavior has a better match with a quasi-linear viscoelastic model. Further, at the forces we were working at  $5.5N$ , it is very possible that there were non-linear effects on the finger that were not modeled. In our model of skin mechanics, we assumed that the rubber and skin form one continuous layer with identical modulus of elasticity. It is known that this is not true. There is actually a discontinuity between the skin and the rubber which our model does not take into account.

## 6 Conclusion

We have shown that tactile perception has a memory effect which is highly correlated with a finger's measured viscoelastic response. We assumed that the finger behaved linearly, but a better model might be Fung's quasi-linear viscoelastic model. The viscoelastic mechanical and perceptual effects vary by almost a factor of two over our subjects. Improved apparatus is needed to measure the memory perceptual effects for dynamic patterns.

## References

- [1] M. Cohn, M. Lam, and R.S. Fearing. Tactile feedback for teleoperation. *Telem manipulator Technology-SPIE Proceedings 1833*, 1992.
- [2] C.L. Van Doren. A model of spatiotemporal tactile sensitivity linking psychophysics to tissue mechanics. *Journal of Acoustical Society of America*, 85(5):2065–2080, 1989.
- [3] C.L. Van Doren. The effects of a surround on vibrotactile thresholds: Evidence for spatial and temporal independence in the non-Pacinian I (NPI) channel. *Journal of Acoustical Society of America*, 87(6):2655–2661, 1990.
- [4] R.S. Fearing. Tactile sensing mechanisms. *The International Journal of Robotics Research*, 9(3):3–23, 1990.
- [5] R.S. Fearing and John M. Hollerbach. Basic solid mechanics for tactile sensing. *The International Journal of Robotics Research*, 4(3):40–54, 1985.
- [6] Y.C. Fung. *Biomechanics: Mechanical Properties of Living Tissues*. Springer-Verlag, second edition, 1993.
- [7] R.D. Howe, April 1997. Personal communication.
- [8] R.S. Johansson, U. Landstrom and R. Lundstrom, "Responses of Mechanoreceptive Afferent Units in the Glabrous Skin of the Human Hand to Sinusoidal Displacements", *Brain Research*, vol. 244, p. 17-25, 1982.
- [9] K.L. Johnson, *Contact Mechanics*, Cambridge University Press, 1985.
- [10] D.A. Kontarinis, May 1995. Harvard University, PhD Thesis.
- [11] E.J. Nicolson. Standardizing I/O for mechatronic systems (sioms) using real time unix device drivers. *IEEE Int. Conf. on Robotics and Automation*, 1994.
- [12] D. Pawluk and R.D. Howe. Dynamic contact mechanics of the human fingerpad, part ii: Distributed response. Technical report 96-004, Harvard Robotics Lab, 1996.
- [13] D. Pawluk and R.D. Howe. Dynamic contact mechanics of the human fingerpad, part i: Lumped response. *Submitted to Journal of Biomechanical Engineering*, 1996.
- [14] D. Pawluk and R.D. Howe. A viscoelastic model of the human fingerpad. Technical report 96-003, Harvard Robotics Lab, 1996.
- [15] J.R. Phillips and K.O. Johnson. Tactile spatial resolution III. a continuum mechanics model of skin predicting mechanoreceptor responses to bars, edges, and gratings. *Journal of Neurophysiology*, 46(6):1204–1225, 1981.
- [16] E.R. Serina, C.D. Mote Jr., and D.M. Rempel. Mechanical properties of the fingertip pulp under repeated, dynamic, compressive loading. *ASME Winter Annual Meeting*, 1995.
- [17] E.M. Sladek and R.S. Fearing, "The Dynamic Response of a Tactile Sensor", *IEEE Int. Conf. on Robotics and Automation*, Cincinnati, OH May 1990.
- [18] M.A. Srinivasan and K. Dandekar, "An Investigation of the Mechanics of Tactile Sense Using Two Dimensional Models of the Primate Fingertip" *Jnl. of Biomechanical Engineering (trans. of the ASME)*, vol. 118, pp. 48-55, 1996.
- [19] E. Tan, August 1995. UC Berkeley, M.S. Thesis.
- [20] R. Walpole and R. Myers. *Probability and Statistics for Engineers and Scientists*. Macmillan Publishing Company, fifth edition, 1993.